RSC Advances

PAPER

View Article Online
View Journal | View Issue



Cite this: *RSC Adv.*, 2025, **15**, 13618

# Evaluation of the interactions of hydrazide derivatives with acetic acid and molecular modeling analysis of *N*-acetylated hydrazides†

Hamid Beyzaei, * Sakineh Sheikh, Fereshteh Shiri* and Reza Aryan

Acetic acid, as a weak organic acid, has a wide range of food, pharmaceutical, and industrial applications. It is also used as a green solvent, catalyst, and reagent in chemical experiments. Properties such as non-toxicity, safety, availability, and low cost have made it the preferred choice for acetylation processes. In this project, the interactions of a series of alkyl/aryl/heteroaryl hydrazides with acetic acid were investigated under reflux heating. A variety of reactions, including *C*- and *N*-acetylation, hydrolysis, and rearrangement, occurred in the presence of acetic acid. Most of the products were recrystallized in good to excellent yields under these conditions without the need for further purification. All synthesized compounds were characterized by NMR ($^{1}$H and $^{13}$C), FT-IR, and CHNS analysis. In addition, a novel method was proposed for the preparation of products **2a** and **2i–q**. This method has the potential to be extended to similar reagents. To investigate the biological activity and drug-like properties, some *in silico* methods were employed on the synthesized compounds. Screening using the ChEMBL database revealed that out of 17 synthesized compounds, compounds **2b** (ChEMBL93746), **2c** (ChEMBL22425), and **2d** (ChEMBL441343) exhibited significant activity against targets SIRT1, TPMT, and Tyrosinase, with measured values below 200 μM. Molecular docking demonstrated that compound **2o** interacted with all three targets. These findings provide valuable insights into its potential as a promising multi-target drug candidate for future investigations.

Received 21st February 2025
Accepted 7th April 2025

DOI: 10.1039/d5ra01286d

rsc.li/rsc-advances



## 1 Introduction

Acetic acid is an aliphatic carboxylic acid with a p$K_a$ of 4.76. The characteristic odor of vinegar is due to the presence of about 4–6% of this monoprotic acid, which is why it is also known as vinegar acid. Pure acetic acid, known as glacial acetic acid in laboratory grade, is a colorless and corrosive liquid with a boiling point of 117–118 °C. Acetic acid is a byproduct of carbohydrate fermentation and of the destructive distillation of wood. *Acetobacter* and *Gluconobacter*, two main groups of Gram-negative aerobic acetic acid bacteria, oxidize carbohydrates first to ethanol and then to acetic acid.[1] In addition to gluconic acid and acetic acid, other organic acids and products, such as ketones, can also be produced as a result of the enzymatic activity of these bacteria. Acetic acid bacteria are also efficient microorganisms in the production of cellulose and sorbose.[2,3]

Acetic acid can inhibit the growth of a variety of pathogenic bacterial and fungal strains, which is why it is used as a food preservative and a local antiseptic agent.[4] Irrigation of nosocomial and burn wounds with acetic acid is one of the most effective and common methods to prevent microbial infections.[5,6] This medicinal agent is used to flush the urinary bladder,[7] manage soft tissue injuries *via* iontophoresis,[8] treat external otitis,[9] remove ear wax,[10] and for visual inspection of the cervix in office cervicoscopy and stationary colposcopy.[11] In organic synthesis, it is applied as a solvent (reaction medium or recrystallization process), reagent, and catalyst in organic reactions.[12–15]

The hydrazide functional group (–C(=O)NR$^1$NR$^2$R$^3$) is present in a wide range of biologically active compounds.[16] Isoniazid (isonicotinic acid hydrazide), an antibiotic, treats mycobacterial infections, especially tuberculosis. This tuberculostatic agent interferes with the biosynthesis of *Mycobacterium tuberculosis* through inhibition of enoyl-acyl carrier protein reductase (InhA).[17] Tecovirimat is a P37 protein inhibitor and blocks its interaction with Rab9 GTPase and TIP47.[18] This antiviral medication is prescribed to treat diseases caused by orthopoxviruses such as monkeypox, smallpox, and cowpox. Cyclooxygenases, precursors of prostaglandins, metabolize arachidonic acid to cyclic endoperoxides. These isoenzymes are inhibited by bumadizone calcium, a non-steroidal antipyretic, anti-inflammatory, and analgesic drug used to treat gout and rheumatoid arthritis.[19] Cilazapril is a commonly prescribed drug to manage hypertension. It is an inhibitor of pyridazine angiotensin I-converting enzyme (ACE/kininase II), blocks the

*Department of Chemistry, Faculty of Science, University of Zabol, Zabol, Iran. E-mail: hbeyzaei@yahoo.com; hbeyzaei@uoz.ac.ir; Fax: +98 54 31232180; Tel: +98 54-31232186*

† Electronic supplementary information (ESI) available. See DOI: https://doi.org/10.1039/d5ra01286d

synthesis of the vasoconstrictor angiotensin II from angiotensin I, and decreases blood pressure.[20]

Diversity in the biological properties of molecules containing the hydrazide functional group motivated us to perform *C*- or *N*-acetylation on some alkyl/aryl/heteroaryl hydrazides using acetic acid. For this purpose, 17 compounds were prepared. All synthesized compounds were assessed *in silico* for their biological activities and drug potential. These theoretical approaches underscore the pharmacological potential of the synthesized compounds and provide a foundation for further optimization.

# 2 Experimental

## 2.1 Materials and methods

All chemicals and solvents were purchased from Sigma-Aldrich and used without further purification. The progress of reactions was monitored by aluminum TLC plates pre-coated with silica gel and a fluorescent indicator (F254). The uncorrected melting points were measured using a Kruss type KSP1N melting point meter. NMR ($^1$H and $^{13}$C) spectra were recorded using a Bruker Avance III 300 MHz spectrometer. FT-IR spectra were collected in KBr disks using a Bruker Tensor 27 FT-IR spectrometer. The elemental composition of the target products was determined using a Thermo Finnigan Flash EA CHNS-O microanalyzer.

## 2.2 General procedure for the reaction of hydrazides with glacial acetic acid

A solution containing 2 mmol of various hydrazides (**1a–r**) in 1 ml of glacial acetic acid was heated under reflux for 2–8 h. The reaction mixture was then cooled to room temperature. Some products crystallized under these conditions, and soluble products were precipitated by adding the reaction solution to crushed ice. The precipitates were filtered off, washed with cold diethyl ether, and oven-dried at 50 °C. If necessary, the final solids were recrystallized from ethanol or an ethanol–water mixture.

**2.2.1 4-Acetylbenzohydrazide (2a).** FT-IR $\nu_{max}$ 3413, 3129, 1673, 1609, 1517, 1398, 1174, 864, 773, 620, 547, 475 cm$^{-1}$; $^1$H NMR (300 MHz, DMSO-$d_6$) $\delta$ 2.10 (s, 3H, $CH_3$), 7.71 (d, $J$ = 8.6 Hz, 2H, H-3,5 Ph), 7.90 (d, $J$ = 8.6 Hz, 2H, H-2,6 Ph), 10.27 (s, 2H, $NH_2$), 12.69 (s, 1H, NH) ppm; $^{13}$C NMR (75 MHz, DMSO-$d_6$) $\delta$ 169.34 ($CH_3C$=O), 167.42 (NHCO), 143.82 (C-4 Ph), 130.86 (C-3,5 Ph), 125. 33 (C-1 Ph), 118.62 (C-2,6 Ph), 24.64 ($CH_3$) ppm; anal. calcd for $C_9H_{10}N_2O_2$ (178.19): C 60.66, H 5.66, N 15.72; found: C 60.60, H 5.62, N 15.77.

**2.2.2 4-(*tert*-Butyl)benzoic acid (2b).** FT-IR $\nu_{max}$ 3512, 3239, 2963, 2358, 1640, 1539, 1499, 1368, 1277, 1122, 1022, 848, 769, 699, 561 cm$^{-1}$; $^1$H NMR (300 MHz, DMSO-$d_6$) $\delta$ 1.34 (s, 9H, 3 × $CH_3$), 7.56 (d, $J$ = 8.4 Hz, 2H, H-3,5 Ph), 7.89 (d, $J$ = 8.4 Hz, 2H, H-2,6 Ph), 10.44 (s, 1H, OH) ppm; $^{13}$C NMR (75 MHz, DMSO-$d_6$) $\delta$ 166.20 (C=O), 155.15 (C-4 Ph), 130.35 (C-1 Ph), 127.88 (C-2,6 Ph), 125.76 (C-3,5 Ph), 35.19 ($C(CH_3)_3$), 31.41 ($CH_3$) ppm; anal. calcd for $C_{11}H_{14}O_2$ (178.23): C 74.13, H 7.92; found: C 74.16, H 7.92.

**2.2.3 3-Methoxybenzoic acid (2c).** FT-IR $\nu_{max}$ 3514, 3236, 1636, 1581, 1537, 1480, 1289, 1045, 804, 740, 681 cm$^{-1}$; $^1$H NMR (300 MHz, DMSO-$d_6$) $\delta$ 3.85 (s, 3H, $CH_3$), 7.18 (m, 1H, H-4 Ph), 7.43–7.55 (m, 3H, H-2,5,6 Ph), 10.50 (br s, 1H, OH) ppm; $^{13}$C NMR (75 MHz, DMSO-$d_6$) $\delta$ 166.95 (C=O), 159.69 (C-3 Ph), 134.49 (C-1 Ph), 130.17 (C-5 Ph), 120.15 (C-6 Ph), 118.19 (C-4 Ph), 112.98 (C-2 Ph), 55.78 ($CH_3$) ppm; anal. calcd for $C_8H_8O_3$ (152.15): C 63.15, H 5.30; found: C 63.20, H 5.33.

**2.2.4 4-Hydroxybenzoic acid (2d).** FT-IR $\nu_{max}$ 3741, 3390, 2668, 2549, 2362, 1681, 1601, 1549, 1513, 1416, 1285, 1240, 1164, 1111, 1013, 931, 849, 772, 690, 651, 614, 544, 499 cm$^{-1}$; $^1$H NMR (300 MHz, DMSO-$d_6$) $\delta$ 6.83 (d, $J$ = 8.4 Hz, 2H, C-3,5 Ph), 7.81 (d, $J$ = 8.4 Hz, 2H, C-2,6 Ph), 11.02 (brs, 2H, 2 × OH) ppm; $^{13}$C NMR (75 MHz, DMSO-$d_6$) $\delta$ 169.10 (C=O), 161.95 (C-4 Ph), 131.95 (C-2,6 Ph), 122.48 (C-1 Ph), 115.51 (C-3,5 Ph) ppm; anal. calcd for $C_7H_6O_3$ (138.12): C 60.87, H 4.38; found: C 60.91, H 4.39.

**2.2.5 Isonicotinic acid (2e).** FT-IR $\nu_{max}$ 3512, 1645, 1545, 1296, 752, 701 cm$^{-1}$; $^1$H NMR (300 MHz, DMSO-$d_6$) $\delta$ 7.85 (d, $J$ = 6.0 Hz, 2H, H-3,5 Py), 8.83 (d, $J$ = 6.0 Hz, 2H, H-2,6 Py), 11.01 (brs, 1H, OH) ppm; $^{13}$C NMR (75 MHz, DMSO-$d_6$) $\delta$ 164.77 (C=O), 151.03 (C-2,6 Py), 139.77 (C-4 Py), 121.80 (C-3,5 Py) ppm; anal. calcd for $C_6H_5NO_2$ (123.11): C 58.54, H 4.09, N 11.38; found: C 58.58, H 4.11, N 11.33.

**2.2.6 Nicotinic acid (2f).** FT-IR $\nu_{max}$ 3741, 2363, 1712, 1593, 1413, 1318, 1177, 1032, 817, 751, 689, 636 cm$^{-1}$; $^1$H NMR (300 MHz, DMSO-$d_6$) $\delta$ 7.52 (m, 1H, H-5 Py), 8.27 (d, $J$ = 7.8 Hz, 1H, H-4 Py), 8.77 (m, 1H, H-6 Py), 9.09 (s, 1H, H-2 Py), 13.02 (brs, 1H, OH) ppm; $^{13}$C NMR (75 MHz, DMSO-$d_6$) $\delta$ 166.78 (C=O), 153.58 (C-6 Py), 150.67 (C-2 Py), 137.41 (C-4 Py), 127.15 (C-3 Py), 124.18 (C-5 Py); anal. calcd for $C_6H_5NO_2$ (123.11): C 58.54, H 4.09, N 11.38; found: C 58.50, H 4.12, N 11.38.

**2.2.7 Acetohydrazide (2g).** FT-IR $\nu_{max}$ 3225, 1688, 1268, 1015, 631, 545 cm$^{-1}$; $^1$H NMR (300 MHz, DMSO-$d_6$) $\delta$ 1.83 (s, 3H, $CH_3$), 7.47 (brs, 2H, $NH_2$), 9.79 (s, 1H, NH) ppm; $^{13}$C NMR (75 MHz, DMSO-$d_6$) $\delta$ 168.74 (C=O), 20.93 ($CH_3$) ppm; anal. calcd for $C_2H_6N_2O$ (74.08): C 32.43, H 8.16, N 37.81; found: C 32.39, H 8.19, N 37.77.

**2.2.8 Acetamide (2h).** FT-IR $\nu_{max}$ 3052, 1697, 1420, 1315, 1203, 923, 805, 637, 578 cm$^{-1}$; $^1$H NMR (300 MHz, DMSO-$d_6$) $\delta$ 2.42 (s, 3H, $CH_3$), 12.25 (brs, 2H, $NH_2$) ppm; $^{13}$C NMR (75 MHz, DMSO-$d_6$) $\delta$ 174.28 (C=O), 29.52 ($CH_3$) ppm; anal. calcd for $C_2H_5NO$ (59.07): C 40.67, H 8.53, N 23.71; found: C 40.70, H 8.54, N 23.73.

**2.2.9 *N*′-Acetyl-4-nitrobenzohydrazide (2i).** FT-IR $\nu_{max}$ 3515, 3216, 2360, 1693, 1588, 1514, 1471, 1351, 1270, 1107, 1003, 867, 714, 648 cm$^{-1}$; $^1$H NMR (300 MHz, DMSO-$d_6$) $\delta$ 1.97 (s, 3H, $CH_3$), 8.11 (d, $J$ = 7.2 Hz, 2H, H-2,6 Ph), 8.35 (d, $J$ = 7.2 Hz, 2H, H-3,5 Ph), 10.08, 10.81 (brs, 2H, 2 × NH) ppm; $^{13}$C NMR (75 MHz, DMSO-$d_6$) $\delta$ 169.97 ($HC_3C$=O), 164.40 (Ph-$C$=O), 149.78 (C-4 Ph), 138.63 (C-1 Ph), 129.43 (C-2,6 Ph), 124.13 (C-3,5 Ph), 21.02 ($CH_3$) ppm; anal. calcd for $C_9H_9N_3O_4$ (223.19): C 48.43, H 4.06, N 18.83; found: C 48.39, H 4.12, N 18.78.

**2.2.10 *N*′-Acetyl-4-fluorobenzohydrazide (2j).** FT-IR $\nu_{max}$ 3515, 1660, 1620, 1512, 1424, 1335, 1141, 832, 733 cm$^{-1}$; $^1$H NMR (300 MHz, DMSO-$d_6$) $\delta$ 2.03 (s, 3H, $CH_3$), 7.25 (d, $J$ = 9.6 Hz, 2H, H-3,5 Ph), 8.85 (d, $J$ = 9.6 Hz, 2H, H-2,6 Ph), 10.07, 10.44 (brs, 2H, 2 × NH) ppm; $^{13}$C NMR (75 MHz, DMSO-$d_6$) $\delta$ 169.46 ($HC_3C$=O), 149.02 (Ph-$C$=O), 137.07 (C-4 Ph), 129.99

(C-1 Ph), 123.58 (C-2,6 Ph), 115.91 (C-3,5 Ph), 21.05 ($CH_3$) ppm; Anal. Calcd for $C_9H_9FN_2O_2$ (196.18): C 55.10, H 4.62, N 14.28; found: C 55.10, H 4.67, N 14.34.

**2.2.11 *N′*-Acetyl-4-(trifluoromethyl)benzohydrazide (2k).** FT-IR $\nu_{max}$ 3513, 2363, 1685, 1549, 1410, 1285, 1018, 757, 620 $cm^{-1}$; $^1H$ NMR (300 MHz, DMSO-$d_6$) $\delta$ 1.84 (s, 3H, $CH_3$), 7.33–7.66 (m, 4H, H-2,3,5,6 Ph), 9.76 (s, 2H, 2 × NH) ppm; $^{13}C$ NMR (75 MHz, DMSO-$d_6$) $\delta$ 169.54 ($HC_3C$═O), 165.51 (Ph-$C$═O), 147.39 (C-1 Ph), 136.35 (C-4 Ph), 127.19 (C-2,6 Ph), 125.41 (C-3,5 Ph), 123.75 ($CF_3$), 20.95 ($CH_3$) ppm; anal. calcd for $C_{10}H_9F_3N_2O_2$ (246.19): C 48.79, H 3.68, N 11.38; found: C 48.84, H 3.61, N 11.30.

**2.2.12 *N′*-Acetyl-4-hydroxybenzohydrazide (2l).** FT-IR $\nu_{max}$ 3172, 3018, 1703, 1616, 1568, 1507, 1344, 1278, 1231, 1169, 1041, 1001, 893, 852, 819, 769, 668, 618, 567, 493 $cm^{-1}$; $^1H$ NMR (300 MHz, DMSO-$d_6$) $\delta$ 1.92 (s, 3H, $CH_3$), 6.84 (d, $J$ = 8.7 Hz, 2H, H-3,5 Ph), 7.76 (d, $J$ = 8.7 Hz, 2H, H-2,6 Ph), 9.06 (s, 1H, OH), 9.80, 10.04 (s, 2H, 2 × NH) ppm; $^{13}C$ NMR (75 MHz, DMSO-$d_6$) $\delta$ 169.12 ($HC_3C$═O), 165.71 (Ph-$C$═O), 161.06 (C-4 Ph), 129.92 (C-2,6 Ph), 123.58 (C-1 Ph), 115.42 (C-3,5 Ph), 21.09 ($CH_3$) ppm; anal. calcd for $C_9H_{10}N_2O_3$ (194.19): C 55.67, H 5.19, N 14.43; found: C 55.72, H 5.18, N 14.37.

**2.2.13 *N′*-Acetyl-3-hydroxybenzohydrazide (2m).** FT-IR $\nu_{max}$ 3331, 1650, 1584, 1538, 1491, 1365, 1253, 1168, 994, 857, 799, 747, 673, 555 $cm^{-1}$; $^1H$ NMR (300 MHz, DMSO-$d_6$) $\delta$ 1.94 (s, 3H, $CH_3$), 7.00 (m, 1H, H-2 Ph), 7.26–7.40 (m, 3H, H-4,5,6 Ph), 9.91–10.10 (brs, 3H, OH, 2 × NH) ppm; $^{13}C$ NMR (75 MHz, DMSO-$d_6$) $\delta$ 169.15 ($HC_3C$═O), 166.17 (Ph-$C$═O), 157.89 (C-3 Ph), 134.41 (C-1 Ph), 129.96 (C-5 Ph), 119.21 (C-6 Ph), 118.35 (C-4 Ph), 114.91 (C-2 Ph), 21.07 ($CH_3$); anal. calcd for $C_9H_{10}N_2O_3$ (194.19): C 55.67, H 5.19, N 14.43; found: C 55.67, H 5.23, N 14.46.

**2.2.14 *N′*-Acetyl-3-bromobenzohydrazide (2n).** FT-IR $\nu_{max}$ 3431, 1642, 1556, 1296, 735 $cm^{-1}$; $^1H$ NMR (300 MHz, DMSO-$d_6$) $\delta$ 1.95 (s, 3H, $CH_3$), 7.50 (m, 1H, H-5 Ph), 7.79–7.94 (m, 2H, H-4,6 Ph), 8.09 (m, 1H, H-2 Ph), 10.01–10.62 (brs, 2H, 2 × NH) ppm; $^{13}C$ NMR (75 MHz, DMSO-$d_6$) $\delta$ 169.01 ($HC_3C$═O), 164.53 (Ph-$C$═O), 135.03 (C-1 Ph), 131.36 (C-5 Ph), 131.25 (C-2 Ph), 130.58 (C-4 Ph), 127.02 (C-6 Ph), 122.23 (C-3 Ph), 21.07 ($CH_3$) ppm; anal. calcd for $C_9H_9BrN_2O_2$ (257.09): C 42.05, H 3.53, N 10.90; found: C 42.12, H 3.49, N 10.89.

**2.2.15 *N′*-Acetyl-3-hydroxy-2-naphthohydrazide (2o).** FT-IR $\nu_{max}$ 3026, 1601, 1492, 1359, 1271, 1218, 1162, 1001, 912, 874, 744, 701, 655, 592, 467 $cm^{-1}$; $^1H$ NMR (300 MHz, DMSO-$d_6$) $\delta$ 2.03 (s, 3H, $CH_3$), 7.37 (m, 2H, H–Np), 7.51 (m, 1H, H–Np), 7.77 (d, $J$ = 8.3 Hz, 1H, H–Np), 7.92 (d, $J$ = 8.3 Hz, 1H, H–Np), 8.59 (s, 1H, H–Np), 10.49, 10.82 (brs, 2H, 2 × NH), 11.57 (s, 1H, OH) ppm; $^{13}C$ NMR (75 MHz, DMSO-$d_6$) $\delta$ 169.08 ($HC_3C$═O), 165.51 (Np-$C$═O), 154.48 (C-3 Np), 136.49 (C-4a Np), 131.18 (C-8a Np), 129.29 (C-1 Np), 128.86 (C-8 Np), 127.27 (C-6 Np), 126.29 (C-5 Np), 124.34 (C-7 Np), 118.96 (C-2 Np), 111.24 (C-4 Np), 20.96 ($CH_3$) ppm; anal. calcd for $C_{13}H_{12}N_2O_3$ (244.25): C 63.93, H 4.95, N 11.47; found: C 70.01, H 4.97, N 11.44.

**2.2.16 *N′*-Acetylthiophene-2-carbohydrazide (2p).** FT-IR $\nu_{max}$ 3742, 3516, 3211, 3012, 2361, 1688, 1629, 1548, 1419, 1365, 1286, 1097, 1002, 846, 723, 608 $cm^{-1}$; $^1H$ NMR (300 MHz, DMSO-$d_6$) $\delta$ 1.94 (s, 3H, $CH_3$), 7.22 (m, 1H, H-4 Th), 7.84–7.92 (m, 2H, H-3,5 Th), 10.35, 10.59 (s, 2H, 2 × NH) ppm; $^{13}C$ NMR (75 MHz, DMSO-$d_6$) $\delta$ 169.20 ($HC_3C$═O), 161.02 (Th-$C$═O), 137.82 (C-2 Th), 132.02 (C-3 Th), 129.32 (C-5 Th), 128.60 (C-4 Th), 21.04 ($CH_3$); anal. calcd for $C_7H_8N_2O_2S$ (184.21): C 45.64, H 4.38, N 15.21, S 17.40; found: C 45.66, H 4.35, N 15.23, S 17.33.

**2.2.17 *N′*-Acetylacetohydrazide (2q).** FT-IR $\nu_{max}$ 3224, 1600, 1506, 1432, 1364, 1258, 1017, 921, 638, 550, 473 $cm^{-1}$; $^1H$ NMR (300 MHz, DMSO-$d_6$) $\delta$ 1.85 (s, 6H, 2 × $CH_3$), 10.29 (brs, 2H, 2 × NH) ppm; $^{13}C$ NMR (75 MHz, DMSO-$d_6$) $\delta$ 173.76 (2 × C═O), 22.77 (2 × $CH_3$) ppm; anal. calcd for $C_4H_8N_2O_2$ (116.12): C 41.37, H 6.94, N 24.13; found: C 41.33, H 6.92, N 24.10.

### 2.3 Molecular modeling

Computer simulation was applied to provide valuable insights into structure–activity relationships (SAR) for optimizing lead compounds. Seventeen synthesized compounds were assessed for their biological activity and drug potential through database screening on ChEMBL[21] and ADMET profiling (absorption, distribution, metabolism, excretion, and toxicity).[22] Molecular docking was performed to evaluate the binding affinity and predict potential protein binding sites for the synthesized compounds.[23] The docking simulations were carried out using the Smina program on the crystal structures of the targets SIRT1 (PDB ID: 4ZZH), TPMT (PDB ID: 2BZG), and tyrosinase (PDB ID: 7RK7), obtained from the RCSB Protein Data Bank. Missing residues in the 7RK7 structure were predicted using the AlphaFold web server, employing a homology modeling approach.[24] Prior to docking, bound water molecules and ligands were removed, and polar hydrogens were added to the proteins. The synthesized compounds were prepared by constructing their 3D structures using ChemDraw Pro 23.1.1.3, followed by energy minimization.[25] During docking, the ligand molecules were treated as flexible, with binding poses and torsions sampled using the biased probability Monte Carlo minimization technique, which combines random conformational changes with local energy optimization.[26] The best binding modes were selected based on the lowest energy conformations calculated by the Smina scoring function. Docking results were analyzed and visualized using BIOVIA Discovery Studio Client 2024. Forecasting ADMET properties is a critical yet complex step in the optimization of lead compounds during the drug discovery process. To evaluate these properties for the synthesized compounds, predictions were carried out using SwissADME and DataWarrior software tools.[27]

## 3 Results and discussion

### 3.1 Chemistry

Acetic acid is an organic acid primarily derived from natural sources. It is considered as a green compound due to its properties, such as high solubility in water, biodegradability, biocompatibility, and non-toxic nature. The acetate anion, the conjugate base of acetic acid, serves as a building block in the biosynthesis of various macronutrients. In this study, acetic acid was used as an environmentally friendly substrate to react with hydrazides under reflux conditions (Scheme 1 and Table 1).

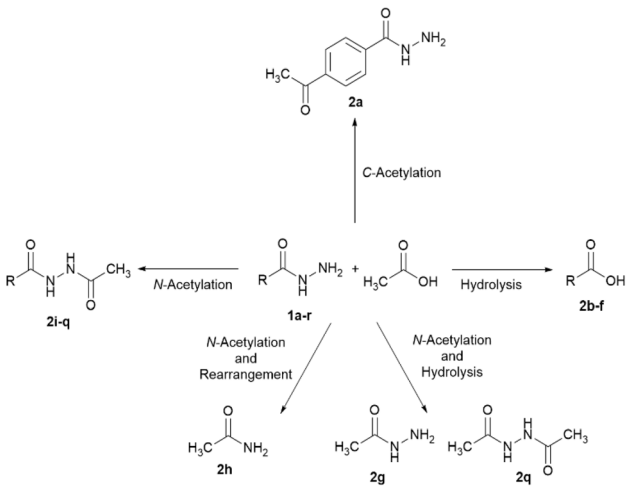


Scheme 1 Various interactions of acetic acid with alkyl/aryl/heteroaryl hydrazides.

As shown in Scheme 1, hydrazide derivatives **1a–r** reacted differently with acetic acid. *C*-acetylation was observed only in hydrazide **1a**. Benzohydrazide (**1a**) underwent acetylation at the para position, despite the electron-withdrawing and meta-directing nature of the –$CONHNH_2$ group. Product **2a** had been previously synthesized *via* the reaction of ethyl 4-acetylbenzoate with hydrazine hydrate in 73% yield.[28] Hydrazides **1b–f** were hydrolyzed to the corresponding carboxylic acids **2b–f** in the presence of acetic acid.

4-(Dimethylamino)benzohydrazide (**1g**) and formic hydrazide (**1h**) were initially *N*-acetylated. Product **2g** was obtained through the hydrolysis of its *N*-acetylated intermediate. *N*′-Formylacetohydrazide (I) underwent rearrangement to acetamide (**2h**) and isocyanic acid (II), which was then hydrolyzed to carbamic acid (III) and decomposed into ammonia and carbon dioxide (Scheme 2).

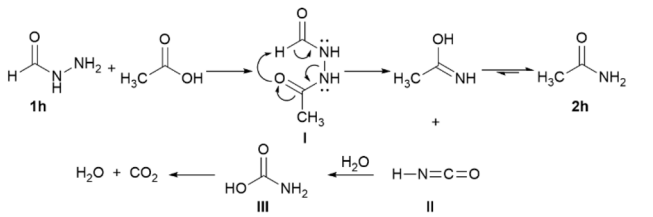


Scheme 2 Proposed mechanism for the formation of acetamide from formic hydrazide.

Hydrazides **1i–q** were acetylated on their $NH_2$ groups to yield *N*′-acetyl hydrazides **2i–q**. These products have been prepared *via* *N*-acetylation of aryl hydrazides using acetylating reagents such as acetyl chloride, acetic anhydride, and acetyl arenoates, as well as *N*-acetylation of acetohydrazide using aroyl chlorides or aryl carboxylic acids (Scheme 3).[29–33,35–37]

*N*′-Acetylacetohydrazide (**2q**) was produced *via* the initial *N*-acetylation of both acetohydrazide (**1q**) and phenylacetic hydrazide (**1r**). Subsequent hydrolysis of the *N*-acetylated intermediate of hydrazide **1r** and re-acetylation afforded product **2q**. This product has been primarily synthesized *via* three routes (Scheme 4): (A) the reaction of hydrazine hydrate with common acetylating agents;[35] (B) *N*-acetylation of acetohydrazide;[38] (C) dehydrogenative N–N coupling of acetamide.[39]

The chemical structures of products **2a–q** were confirmed by physical and spectral data. In $^1$H NMR spectroscopy, a doublet of doublets at $\delta$ 7.71 and 7.90 ppm defined the *para*-substitution pattern of product **2a.** Singlet or broad peaks in the range of 10.44–13.02 ppm corresponded to the hydroxyl group of carboxylic acids **2b–f**. Surprisingly, the 2-hydroxyl group of the aryl ring in hydrazide **1d** was removed in the final product **2d**. Two separate signals at 7.47 and 9.79 ppm were attributed to the $NH_2$ and NH protons of hydrazide **2g**, respectively, while in compound **2h**, a peak at 12.25 ppm corresponded to the amidic $NH_2$ protons. In *N*-acetylated products **2i–q**, protons of the two NH groups appeared at

Table 1 Products formed in the reaction of hydrazides 1a-r and acetic acid

| Entry | R | Product | Time, h | Yield, % | m.p. (lit.), °C |
|---|---|---|---|---|---|
| 1 | $C_6H_5$ | **2a** | 3 | 83.1 | 214–215 (206–208)[28] |
| 2 | 4-*t*-Bu-$C_6H_4$ | **2b** | 8 | 72.4 | 168–169 (162–165) [Sigma-Aldrich] |
| 3 | 3-$CH_3O$-$C_6H_4$ | **2c** | 6 | 73.6 | 115–116 (105–107) [Sigma-Aldrich] |
| 4 | 2,4-$(HO)_2$–$C_6H_3$ | **2d** | 10 | 84.5 | 204–206 (213–217) [Sigma-Aldrich] |
| 5 | Pyridine-4-yl | **2e** | 4 | 71.9 | >300 (315–319) [Sigma-Aldrich] |
| 6 | Pyridine-3-yl | **2f** | 7 | 98.2 | 228–230 (234–238) [Sigma-Aldrich] |
| 7 | 4-$(CH_3)_2N$-$C_6H_4$ | **2g** | 9 | 77.6 | 71–73 (58–68) [Sigma-Aldrich] |
| 8 | H | **2h** | 9 | 95.6 | 84–85 (78–80) [Sigma-Aldrich] |
| 9 | 4-$O_2N$-$C_6H_4$ | **2i** | 3 | 91.9 | 225–227 (240–241)[29] |
| 10 | 4-F-$C_6H_4$ | **2j** | 10 | 81.1 | 196–198 (192–194)[30] |
| 11 | 4-$F_3C$-$C_6H_4$ | **2k** | 10 | 77.3 | 259–261 (Not reported)[31] |
| 12 | 4-HO-$C_6H_4$ | **2l** | 2.5 | 74.2 | 252–253 (250)[32] |
| 13 | 3-HO-$C_6H_4$ | **2m** | 3 | 75.4 | 198–199 (208)[32] |
| 14 | 3-Br-$C_6H_4$ | **2n** | 6.5 | 81.3 | 150–151 (169)[33] |
| 15 | 3-HO-naphthalen-2-yl | **2o** | 8 | 90.9 | 246–248 (234–235)[34] |
| 16 | Thiophen-2yl | **2p** | 10 | 79.7 | 163–165 (178–179)[30] |
| 17 | $CH_3$ | **2q** | 9 | 81.8 | 135–136 (129–130)[35] |
| 18 | $H_5C_6$-$CH_2$ | **2q** | 10 | 75.2 | 135–136 (129–130)[35] |

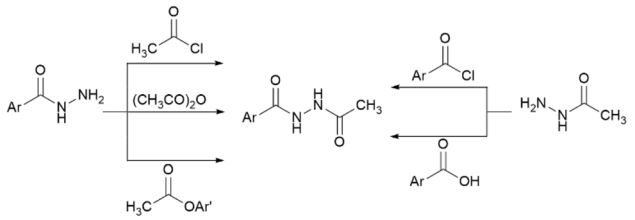

Scheme 3 Synthetic routes of *N*′-acetyl hydrazide derivatives.

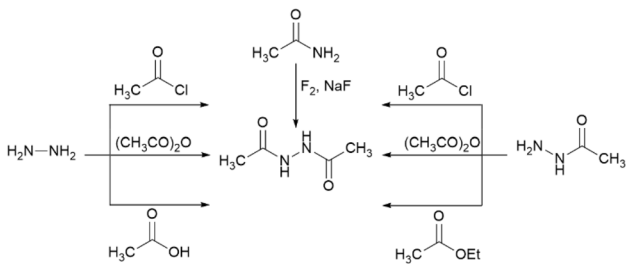

Scheme 4 Selected synthetic routes of *N*′-acetylacetohydrazide.

9.76–10.82 ppm. Additionally, peaks at 164.53–173.76 ppm were assigned to the carbons of their amidic carbonyl groups.

### 3.2 Molecular modeling analysis

**3.2.1 Database screening and molecular docking analysis.** The synthesized compounds were screened in ChEMBL, a manually curated database of bioactive molecules with drug-like properties, to identify any known interactions with the targets. This initial analysis provided a broader chemical and pharmacological context for the compounds. Subsequently, all synthesized compounds were subjected to molecular docking against the identified targets. Among them, compounds **2b** (ChEMBL93746), **2c** (ChEMBL22425), and **2d** (ChEMBL441343) demonstrated significant activity, with **2b** exhibiting an $IC_{50}$ of 200 μM against sirtuin 1 (SIRT1), **2c** showing an $IC_{50}$ of 199 μM against thiopurine methyltransferase (TPMT), and **2d** achieving an $IC_{50}$ of 9.3 μM against tyrosinase. SIRT1 is a nicotinamide adenine dinucleotide ($NAD^+$)-dependent deacetylase that regulates critical cellular processes, including metabolism, stress response, and aging.[40] TPMT catalyzes the methylation of thiopurine drugs, which are widely used to treat autoimmune diseases, certain cancers, and to prevent organ transplant rejection.[41] Tyrosinase, a copper-containing enzyme, is essential for melanin biosynthesis, determining the pigment of skin, hair, and eyes, by catalyzing the oxidation of tyrosine into melanin precursors.[42] Additionally, compounds **2e** (ChEMBL1203), **2f** (ChEMBL573), **2g** (ChEMBL3091859), and **2h** (ChEMBL16081) were found in the ChEMBL database but lack reported activity and specific targets. Notably, compound **2f** (ChEMBL573), identified as niacin or vitamin B3, is an approved drug. Due to the structural similarities and the shared synthesis methodology, all synthesized compounds were docked against the three target proteins: SIRT1, TPMT, and Tyrosinase. Molecular docking aimed to predict the most favorable binding poses of the synthesized compounds within the active sites of the target proteins and identify key residues and binding modes. This approach enabled the identification of protein target candidates associated with the docking poses of the synthesized compounds, which were ranked based on their predicted affinity (see Table 2). Based on Table 2, the predicted affinities indicated that some compounds exhibited more favorable affinities compared to their corresponding compounds reported in the ChEMBL database. For instance, the predicted affinity value of compound **2b** with SIRT1 was $-7.16$ kcal $mol^{-1}$, while compounds **2o** and **2k** demonstrated more favorable energy values. Similarly, TPMT exhibited an affinity of $-7.02$ kcal $mol^{-1}$ with compound **2c**, whereas the nine compounds listed in the table (**2o**, **2k**, **2m**, **2a**, **2n**, **2j**, **2b**, **2l**, and **2i**) demonstrated even more favorable binding energy values in comparison to **2c**. Additionally, tyrosinase showed

Table 2 The docking-predicted minimized affinity of the products for three targets: SIRT1, TPMT and tyrosinase

| Product | Affinity of SIRT1 (kcal $mol^{-1}$) | Product | Affinity of TPMT (kcal $mol^{-1}$) | Product | Affinity of tyrosinase (kcal $mol^{-1}$) |
|---|---|---|---|---|---|
| **2o** | −8.59 | **2o** | −9.62 | **2o** | −8.33 |
| **2k** | −7.76 | **2k** | −8.95 | **2l** | −7.29 |
| **2b** | −7.16 | **2m** | −8.4 | **2m** | −7.28 |
| **2n** | −7.04 | **2a** | −8.35 | **2d** | −6.47 |
| **2a** | −6.97 | **2n** | −8.15 | **2p** | −6.32 |
| **2i** | −6.82 | **2j** | −8.12 | **2j** | −6.16 |
| **2m** | −6.77 | **2b** | −8.07 | **2a** | −5.96 |
| **2j** | −6.7 | **2l** | −8.02 | **2k** | −5.79 |
| **2l** | −6.44 | **2i** | −7.66 | **2b** | −5.79 |
| **2d** | −5.91 | **2c** | −7.02 | **2n** | −5.6 |
| **2c** | −5.67 | **2d** | −6.78 | **2f** | −5.51 |
| **2p** | −5.48 | **2p** | −6.72 | **2i** | −5.38 |
| **2f** | −5.26 | **2f** | −6.36 | **2c** | −5.12 |
| **2e** | −5.13 | **2e** | −6.1 | **2e** | −4.68 |
| **2g** | −4.08 | **2q** | −5.19 | **2g** | −4.27 |
| **2q** | −4.06 | **2g** | −4.23 | **2q** | −3.73 |
| **2h** | −3.15 | **2h** | −3.52 | **2h** | −3.2 |

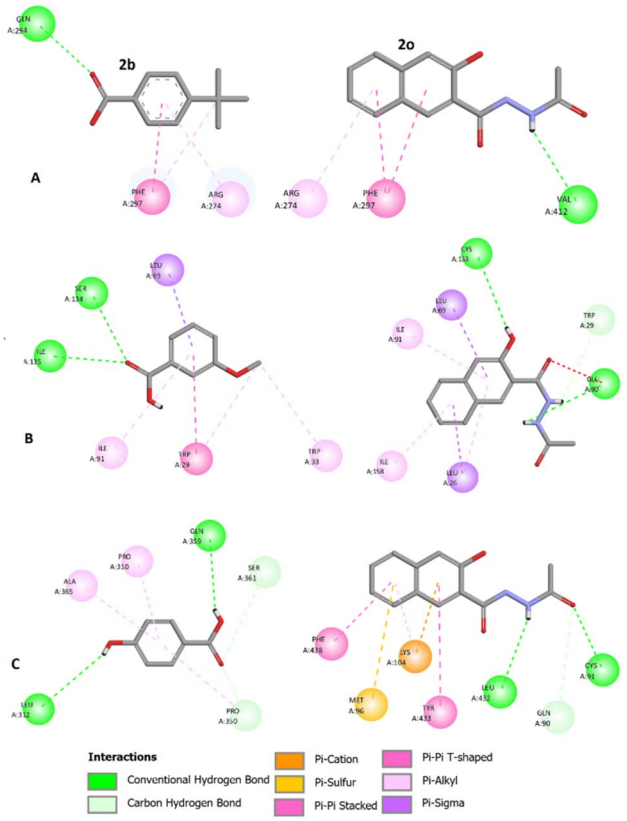


Fig. 1 Molecular docking analysis illustrating the interactions of (A) compounds **2b** and **2o** with SIRT1, (B) compounds **2c** and **2o** with TPMT, and (C) compounds **2d** and **2o** with tyrosinase. The images were generated using Discovery Studio 2024 Client.

better affinities with compounds **2o**, **2l**, and **2m** compared to compound **2d** (−6.47 kcal $mol^{-1}$). Notably, compound **2o** emerged as particularly interesting, as it demonstrated the most favorable affinity across all targets. This suggested its potential as a promising multi-target drug candidate for further investigation.[43–49]

The two-dimensional (2D) ligand–protein interactions of compounds **2b** and **2o** with SIRT1, **2c** and **2o** with TPMT, and **2d** and **2o** with tyrosinase are shown in Fig. 1. In Fig. 1, green dots represent hydrogen bonds, while orange, pink, and purple dots represent hydrophobic interactions. Key residue interactions for each protein with the ligand have been identified and summarized in Table 3. As shown in the docking results (Fig. 1 and Table 3), the biological activity of the compounds appeared to be influenced by several key structural elements that interact with residues. The naphthalene ring system provides a rigid aromatic scaffold that has π–π stacking interactions with aromatic residues in the target. Substituted naphthol or phenolic hydroxyl groups contribute to hydrogen bonding and increase polarity, potentially improving aqueous solubility and binding affinity. Hydrazide groups are capable of acting as hydrogen bond donors and acceptors, thereby facilitating interactions with polar residues at the binding site. Generally, compound **2o** exhibited more interactions with each specific target compared to its corresponding compounds reported in the ChEMBL database.[50–56]

**3.2.2 ADMET predictions.** The use of ADMET analysis facilitates the prediction of the action and behavior of newly synthesized compounds, reducing both costs and time during drug development. The bioavailability radar in SwissADME offers an effective visual tool for assessing drug-likeness by displaying six key descriptive properties at a glance. These properties include lipophilicity (LIPO), molecular size (SIZE), polarity (POLAR), solubility (INSOLU), saturation (INSATU), and molecular flexibility (FLEX). Each descriptor has an optimal range, and molecules that fall within the pink region of the radar are considered to exhibit favourable bioavailability properties in the body. The pink region represents the ideal range for each property as follows: lipophilicity (XLOGP3) between −0.7 and +5.0, molecular weight (MW) between 150 and 500 g $mol^{-1}$, topological polar surface area (TPSA) between 20 and 130 $Å^2$, solubility (log S) no higher than 6, saturation (fraction of carbons in $sp^3$ hybridisation) not less than 0.25, and flexibility with no more than nine rotatable bonds. Table 4 illustrates the bioavailability radar for the synthesized compounds. An analysis of these radars highlights the unsaturation characteristics of the majority of the compounds. When the unsaturation value of a compound exceeds the boundary of the pink region in the radar, it indicates that the degree of unsaturation is beyond the acceptable range. Consequently, the INSATU parameter will require optimization. This deviation could adversely affect key properties such as solubility, stability, and bioavailability. The toxicity risk of the synthesized compounds was assessed using Data Warrior, a widely used computational tool for predicting potential adverse effects of chemical compounds. This evaluation focused on identifying the likelihood of four specific toxicological risks: mutagenicity, tumorigenicity, irritancy, and reproductive toxicity. Mutagenicity indicates the potential of a compound to induce genetic mutations, which could lead to serious health implications, including cancer. Tumorigenicity refers to the compound's potential to promote tumor formation. Irritancy evaluates the potential of the compound to cause

Table 3 Interaction of each protein with the ligands

| Complex | Hydrogen bonds | Hydrophobic interactions |
|---|---|---|
| SIRT1-2b | GLN294 | PHE297, ARG274 |
| SIRT1-2o | VAL412 | PHE297, ARG274 |
| TPMT-2c | SER134, ILE135 | TRP29, TRP33, ILU69, ILU91 |
| TPMT-2o | GLU90, CYS133, TRP29 | LEU26, LEU69, ILU91, ILU158 |
| Tyrosinase-2d | LEU312, PRO350, GLN359, SER361 | PRO310, ALA365 |
| Tyrosinase-2o | GLN90, CYS91, LEU432 | MET96, LYS104, TYR433, PHE438 |

Table 4 Bioavailability radar for the synthesized compounds: a visual overview of drug-likeness with optimal ranges highlighted in pink

| Product | Radar graph | Product | Radar graph |
|---|---|---|---|
| **2a** | 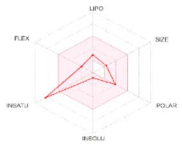 | **2j** | 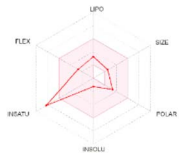 |
| **2b** |  | **2k** |  |
| **2c** | 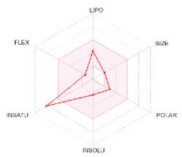 | **2l** | 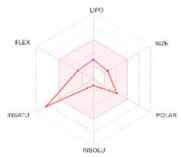 |
| **2d** | 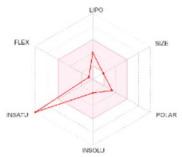 | **2m** | 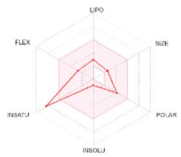 |
| **2e** | 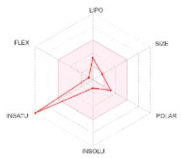 | **2n** | 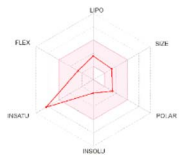 |
| **2f** | 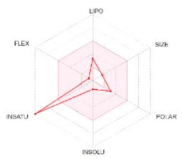 | **2o** |  |
| **2g** |  | **2p** | 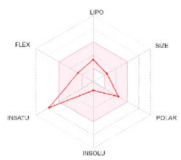 |
| **2h** |  | **2q** |  |
| **2i** |  | | |

irritation upon contact with biological tissues, such as skin or mucous membranes. Lastly, reproductive toxicity assesses the potential of the compound to negatively impact reproductive health, including effects on fertility or embryonic development. The results in Table 5 indicate that only compounds **2h** and **2g** exhibit a high risk for some of the evaluated toxicity parameters, which will be further investigated.

Table 5 Toxicity testing for the synthesized compounds

| Product | Mutagenic | Tumorigenic | Reproductive effective | Irritant |
|---|---|---|---|---|
| **2a** | None | Low | None | None |
| **2b** | None | None | Low | Low |
| **2c** | None | None | None | None |
| **2d** | High | None | None | None |
| **2e** | None | None | None | None |
| **2f** | None | None | None | None |
| **2g** | High | High | None | None |
| **2h** | High | High | High | None |
| **2i** | None | None | Low | None |
| **2j** | None | None | Low | None |
| **2k** | None | None | Low | None |
| **2l** | None | None | Low | None |
| **2m** | None | None | Low | None |
| **2n** | None | None | Low | None |
| **2o** | None | None | Low | None |
| **2p** | None | None | Low | None |
| **2q** | None | None | Low | None |

## 4 Conclusions

Acetic acid is a non-toxic, low cost, water-soluble, accessible, eco-friendly, and biodegradable compound with a variety of applications. It was used as a green solvent in the reactions and recrystallization processes. Small amounts of acid have been shown to facilitate the reaction progress. Despite its lower reactivity, it is safer and cheaper than other acetylating agents such as acetyl chloride, acetic anhydride, and ethyl acetate. In this research, a series of hydrazides reacted with acetic acid under reflux. Acetic acid, in addition to its role as a reaction and recrystallization solvent, acted as an acetylating agent and catalyst. It easily *N*-acetylated hydrazides **1i–r** without the need for carbodiimides. Several unexpected reactions were observed. The novel method offered for preparing products **2a** and **2i–q** occurred under safer, greener, and cheaper conditions compared to previous methods. Molecular modeling and ChEMBL database screening showed that several newly synthesized compounds had promising inhibitory activity against SIRT1, TPMT, and tyrosinase. Among them, compound **2o** stood out with its strong multi-target affinity. The valuable results obtained from this research encourage us to investigate the interaction of equivalent reagents with acetic acid in the future. In addition, molecular modeling findings suggest that further development of the synthesized compounds, especially **2o**, could lead to promising multi-target drug candidates.

## Data availability

The datasets generated during and/or analyzed during the current study are available from the corresponding authors upon reasonable request.

## Author contributions

Hamid Beyzaei: supervision, formal analysis, writing – original draft, writing – review & editing, funding acquisition; Sakineh Sheikh: methodology, investigation; Fereshteh Shiri: supervision, writing – review & editing, conceptualization, software; Reza Aryan: investigation, data curation.

## Conflicts of interest

There are no conflicts to declare.

## Acknowledgements

This work was funded by the University of Zabol (grant number UOZ-GR-4711).

## References

1 K. Zhang, T. T. Zhang, R. R. Guo, Q. Ye, H. L. Zhao and X. H. Huang, The regulation of key flavor of traditional fermented food by microbial metabolism: A review, *Food Chem.:X*, 2023, **19**, 100871.
2 M. Gullo, S. La China, P. M. Falcone and P. Giudici, Biotechnological production of cellulose by acetic acid bacteria: current state and perspectives, *Appl. Microbiol. Biotechnol.*, 2018, **102**, 6885–6898.
3 L. Liu, Y. Chen, S. Yu, J. Chen and J. Zhou, Enhanced production of l-sorbose by systematic engineering of dehydrogenases in Gluconobacter oxydans, *Synth. Syst. Biotechnol.*, 2022, **7**, 730–737.
4 K. M. Park, H. J. Kim, J. Y. Choi and M. Koo, Antimicrobial effect of acetic acid, sodium hypochlorite, and thermal treatments against psychrotolerant bacillus cereus group isolated from lettuce (Lactuca sativa L.), *Foods*, 2021, **10**, 2165.
5 B. S. Nagoba, S. P. Selkar, B. J. Wadher and R. C. Gandhi, Acetic acid treatment of pseudomonal wound infections–a review, *J. Infect. Public Health*, 2013, **6**, 410–415.
6 R. Imran, T. Hassouna, G. Sur, A. Casey, V. Homer, D. Barton, K. Brock, K. Altarrah and N. Moiemen, Efficacy and optimal dose of acetic acid to treat colonised burns wounds: protocol for a pilot randomised controlled trial, *BMJ Open*, 2023, **13**, e058006.
7 B. H. Bachow, Intravesical acetic acid in combination with prophylactic methenamine and ascorbic acid to decrease the incidence of recurrent urinary tract infections associated with intermittent urinary self-catherization: A case report, *Urol. Case Rep.*, 2021, **35**, 101531.
8 Y. Hashmi, A. K. Zhou, A. Jawaid, A. Y. Zhou, V. Shah, A. Thahir and M. Krkovic, The role of acetic acid in orthopaedic surgery, *J. Perioper. Pract.*, 2022, **32**, 162–166.
9 K. P. Basavaraju and S. K. Ranjani, Efficacy of combination of acetic acid and ciprofloxacin eardrops versus only ciprofloxacin eardrops in achieving dry ears in chronic suppurative otitis media, *Egypt. J. Otolaryngol.*, 2023, **39**, 106.
10 K. Aaron, T. E. Cooper, L. Warner and M. J. Burton, Ear drops for the removal of ear wax, *Cochrane Database Syst. Rev.*, 2018, **7**, CD012171.
11 U. R. Poli, P. D. Bidinger and S. Gowrishankar, Visual inspection with acetic acid (via) screening program: 7 years experience in early detection of cervical cancer and pre-cancers in rural South India, *Indian J. Community Med.*, 2015, **40**, 203–207.
12 M. Sanchez-Sala, O. Vallcorba, C. Domingo and J. A. Ayllon, Acetic acid as a solvent for the synthesis of metal–organic frameworks based on trimesic acid, *Polyhedron*, 2019, **170**, 458–462.
13 I. Bratu, G. Borodi, I. KacsÓ, Z. Moldovan, C. Filip, F. Dragan, M. Vasilescu and S. Simon, New solid form of Norfloxacin: structural studies, *Spectroscopy*, 2011, **25**, 53–62.
14 S. Pasricha and T. M. Rangarajan, Green Acetylation of Primary Aromatic Amines, *Resonance*, 2023, **28**, 325–331.
15 H. Beyzaei, M. Moghaddam-Manesh, R. Aryan, B. Ghasemi and A. Samzadeh-Kermani, Synthesis and in vitro antibacterial evaluation of 6-substituted 4-amino-pyrazolo [3,4-d]pyrimidines, *Chem. Pap.*, 2017, **71**, 1685–1691.
16 S. N. Mali, B. R. Thorat, D. R. Gupta and A. Pandey, Mini-Review of the Importance of Hydrazides and Their Derivatives—Synthesis and Biological Activity, *Eng. Proc.*, 2021, **11**, 21.
17 A. N. Unissa, S. Subbian, L. E. Hanna and N. Selvakumar, Overview on mechanisms of isoniazid action and resistance in Mycobacterium tuberculosis, *Infect. Genet. Evol.*, 2016, **45**, 474–492.
18 S. S. Borisevich, Y. V. Gorokhov and S. G. Arkhipov, Binding Site of Tecovirimat, Inhibitor of the p37 Membrane Protein of Orthopox Viruses, *J. Struct. Chem.*, 2024, **65**, 776–785.
19 S. A. Nour, N. S. Abdelmalak and M. J. Naguib, Novel chewable colon targeted tablets of bumadizone calcium for treatment of ulcerative colitis: Formulation and optimization, *J. Drug Deliv. Sci. Technol.*, 2016, **35**, 172–183.
20 M. Stanisz, Ł. Klapiszewski, D. Moszyński, B. J. Stanisz and T. Jesionowski, Evaluation of cilazapril release profiles with the use of lignin-based spherical particles, *J. Drug Deliv. Sci. Technol.*, 2022, **75**, 103636.
21 A. Gaulton, A. Hersey, M. Nowotka, A. P. Bento, J. Chambers, D. Mendez, P. Mutowo, F. Atkinson, L. J. Bellis, E. Cibrián-Uhalte and M. Davies, The ChEMBL database in 2017, *Nucleic Acids Res.*, 2017, **45**, D945–D954.
22 L. L. Ferreira and A. D. Andricopulo, ADMET modeling approaches in drug discovery, *Drug Discov. Today*, 2019, **24**, 1157–1165.
23 J. B. Ghasemi, A. Abdolmaleki and F. Shiri, Molecular docking challenges and limitations, in *Pharmaceutical Sciences: Breakthroughs in Research and Practice*, Information Resources Management Association, IGI Global, 2017, pp. 770–794.
24 J. Moult, K. Fidelis, A. Kryshtafovych, T. Schwede and M. Topf, Critical assessment of techniques for protein structure prediction, fourteenth round. *CASP 14 Abstract Book*, 2020, pp. 1–344.

25 G. W. Milne, Software review of ChemBioDraw 12.0, *J. Chem. Inf. Model.*, 2010, **50**, 2053.
26 D. R. Koes, M. P. Baumgartner and C. J. Camacho, Lessons learned in empirical scoring with smina from the CSAR 2011 benchmarking exercise, *J. Chem. Inf. Model.*, 2013, **53**, 1893–1904.
27 A. Daina, O. Michielin and V. Zoete, SwissADME: a free web tool to evaluate pharmacokinetics, drug-likeness and medicinal chemistry friendliness of small molecules, *Sci. Rep.*, 2017, **7**, 42717.
28 D. Kerzare, R. Chikhale, R. Bansode, N. Amnerkar, N. Karodia, A. Paradkar and P. Khedekar, Design, synthesis, pharmacological evaluation and molecular docking studies of substituted oxadiazolyl-2-oxoindolinylidene propane hydrazide derivatives, *J. Braz. Chem. Soc.*, 2016, **27**, 1998–2010.
29 D. Conole, T. M. Beck, M. Jay-Smith, M. D. Tingle, C. T. Eason, M. A. Brimble and D. Rennison, Synthesis and methemoglobinemia-inducing properties of benzocaine isosteres designed as humane rodenticides, *Bioorg. Med. Chem.*, 2014, **22**, 2220–2235.
30 T. Fang, Q. Tan, Z. Ding, B. Liu and B. Xu, Pd-catalyzed oxidative annulation of hydrazides with isocyanides: synthesis of 2-amino-1,3,4-oxadiazoles, *Org. Lett.*, 2014, **16**, 2342–2345.
31 P. R. Campodónico, M. E. Aliaga, J. G. Santos, E. A. Castro and R. Contreras, Reactivity of benzohydrazide derivatives towards acetylation reaction. Experimental and theoretical studies, *Chem. Phys. Lett.*, 2010, **488**, 86–89.
32 A. M. El Masri, J. N. Smith and R. T. Williams, Studies in detoxication. 75. Further observations on the metabolism of hydrazides of aromatic acid, *Biochem. J.*, 1958, **68**, 587–592.
33 T. Curtius and E. Portner, Hydrazides and azides of organic acids. XV. Treatise. The hydrazides of m- and p-bromobenzoic acid, *J. Prakt. Chem.*, 1898, (58), 190–205.
34 J. Chen, B. Yang, Q. He, Y. Pan and M. Ying, Hydrazide derivative and application thereof, *CN Pat.*, CN108329232A, 2018.
35 S. Paul, P. Nanda, R. Gupta and A. Loupy, $Ac_2O$–Py/basic alumina as a versatile reagent for acetylations in solvent-free conditions under microwave irradiation, *Tetrahedron Lett.*, 2002, **43**, 4261–4265.
36 Y. Hashizume, K. Sekimata, H. Kubota, H. Yamamoto, Y. Koda, H. Koyama, T. Taguri, T. Sato, A. Tanaka and K. Miyazono, Bmp-signal-inhibiting compound, *US Pat.*, US2019/337926A1, 2019.
37 J. Kim, S. Kang, J. Kang, S. Lee, J. J. Seo and M. Seo, Anti-infective compounds, *WO Pat.*, WO2015/193506A1, 2015.
38 J. K. Rai Deka, B. Sahariah and B. K. Sarma, Understanding the Cis–Trans Amide Bond Isomerization of N,N′-Diacylhydrazines to Develop Guidelines for A Priori Prediction of Their Most Stable Solution Conformers, *J. Org. Chem.*, 2024, **89**, 10419–10433.
39 R. D. Chapman, M. C. Davis and R. Gilardi, A new preparation of gem-bis (difluoramino)-alkanes via direct fluorination of geminal bisacetamides, *Synth. Commun.*, 2003, **33**, 4173–4184.
40 F. Liang, S. Kume and D. Koya, SIRT1 and insulin resistance, *Nat. Rev. Endocrinol.*, 2009, **5**, 367–373.
41 R. M. Weinshilboum, D. M. Otterness and C. L. Szumlanski, Methylation pharmacogenetics: catechol O-methyltransferase, thiopurine methyltransferase, and histamine N-methyltransferase, *Annu. Rev. Pharmacol. Toxicol.*, 1999, **39**, 19–52.
42 S. Sharma, K. Bhatt, R. Shrivastava and A. K. Nadda, Tyrosinase and oxygenases: fundamentals and applications, in *Biotechnology of Microbial Enzymes*, ed., G. Brahmachari, Academic Press, 2023, pp. 323–340.
43 A. Abdolmaleki, F. Shiri and J. B. Ghasemi, Computational multi-target drug design, in *Multi-target Drug Design Using Chem-Bioinformatic Approaches*, ed. K. Roy, Humana Press, 2019, pp. 51–90.
44 A. Milelli, V. Tumiatti, M. Micco, M. Rosini, G. Zuccari, L. Raffaghello, G. Bianchi, V. Pistoia, J. F. Díaz, B. Pera and C. Trigili, Structure–activity relationships of novel substituted naphthalene diimides as anticancer agents, *Eur. J. Med. Chem.*, 2012, **57**, 417–428.
45 S. Makar, T. Saha and S. K. Singh, Naphthalene, a versatile platform in medicinal chemistry: Sky-high perspective, *Eur. J. Med. Chem.*, 2019, **161**, 252–276.
46 C. Platella, E. Napolitano, C. Riccardi, D. Musumeci and D. Montesarchio, Disentangling the structure–activity relationships of naphthalene diimides as anticancer G-quadruplex-targeting drugs, *J. Med. Chem.*, 2021, **64**, 3578–3603.
47 B. X. Li, K. Yamanaka and X. Xiao, Structure–activity relationship studies of naphthol AS-E and its derivatives as anticancer agents by inhibiting CREB-mediated gene transcription, *Bioorg. Med. Chem.*, 2012, **20**, 6811–6820.
48 H. K. El-Mawgoud, A. M. Fouda, M. A. El-Nassag, A. A. Elhenawy, M. Y. Alshahrani and A. M. El-Agrody, Discovery of novel rigid analogs of 2-naphthol with potent anticancer activity through multi-target topoisomerase I & II and tyrosine kinase receptor EGFR & VEGFR-2 inhibition mechanism, *Chem. Biol. Interact.*, 2022, **355**, 109838.
49 A. Shrestha, S. Park, S. Shin, T. M. Kadayat, G. Bist, P. Katila, Y. Kwon and E. S. Lee, Design, synthesis, biological evaluation, structure-activity relationship study, and mode of action of 2-phenol-4,6-dichlorophenyl-pyridines, *Bioorg. Chem.*, 2018, **79**, 1–8.
50 S. Song, H. Lee, Y. Jin, Y. M. Ha, S. Bae, H. Y. Chung and H. Suh, Syntheses of hydroxy substituted 2-phenyl-naphthalenes as inhibitors of tyrosinase, *Bioorg. Med. Chem. Lett.*, 2007, **17**, 461–464.
51 Y. F. Lin, Y. H. Hu, Y. L. Jia, Z. C. Li, Y. J. Guo, Q. X. Chen and H. T. Lin, Inhibitory effects of naphthols on the activity of mushroom tyrosinase, *Int. J. Biol. Macromol.*, 2012, **51**, 32–36.
52 M. Vaezi, Structure and inhibition mechanism of some synthetic compounds and phenolic derivatives as tyrosinase inhibitors: Review and new insight, *J. Biomol. Struct. Dyn.*, 2023, **41**, 4798–4810.

53 J. Wu, D. Zhang, L. Chen, J. Li, J. Wang, C. Ning, N. Yu, F. Zhao, D. Chen, X. Chen and K. Chen, Discovery and mechanism study of SIRT1 activators that promote the deacetylation of fluorophore-labeled substrate, *J. Med. Chem.*, 2013, **56**, 761–780.

54 A. Ghosh, A. Sengupta, G. P. Seerapu, A. Nakhi, E. V. Ramarao, N. Bung, G. Bulusu, M. Pal and D. Haldar, A novel SIRT1 inhibitor, 4bb induces apoptosis in HCT116 human colon carcinoma cells partially by activating p53, *Biochem. Biophys. Res. Commun.*, 2017, **488**, 562–569.

55 G. Bononi, L. Flori, V. Citi, C. Acciai, V. Nocilla, A. Martelli, G. Poli, T. Tuccinardi, C. Granchi, L. Testai and V. Calderone, New Synthetic Analogues of Natural Polyphenols as Sirtuin 1-Activating Compounds, *Pharmaceuticals*, 2022, **15**, 339.

56 D. K. Liscombe, G. V. Louie and J. P. Noel, Architectures, mechanisms and molecular evolution of natural product methyltransferases, *Nat. Prod. Rep.*, 2012, **29**, 1238–1250.